AIAA Guidance & Control Conference July 29-31, 1996

Effects of Modeling Errors on Trajectory Predictions in Air Traffic Control Automation

Michael R. C. Jackson [†]
University of Minnesota and
Honeywell Technology Center

Yiyuan Zhao [‡]
University of
Minnesota

Rhonda Slattery [§]
NASA Ames
Research Center

1 Abstract

Air traffic control automation synthesizes aircraft trajectories for the generation of advisories. Trajectory computation employs models of aircraft performances and weather conditions. In contrast, actual trajectories are flown in real aircraft under actual conditions. Since synthetic trajectories are used in landing scheduling and conflict probing, it is very important to understand the differences between computed trajectories and actual trajectories. This paper examines the effects of aircraft modeling errors on the accuracy of trajectory predictions in air traffic control automation. Three-dimensional point-mass aircraft equations of motion are assumed to be able to generate actual aircraft flight paths. Modeling errors are described as uncertain parameters or uncertain input functions. Pilot or autopilot feedback actions are expressed as equality constraints to satisfy control objectives. A typical trajectory is defined by a series of flight segments with different control objectives for each flight segment and conditions that define segment transitions. A constrained linearization approach is used to analyze trajectory differences caused by various modeling errors by developing a linear time varying system that describes the trajectory errors, with expressions to transfer the trajectory errors across moving segment transitions. A numerical example is presented for a complete commercial aircraft descent trajectory consisting of several flight segments.

[†] Ph.D. candidate, Dept. of Aerospace Engineering and Mechanics, Sr. Research Scientist, Member AIAA

[‡] Assistant Professor, Dept. of Aerospace Engineering and Mechanics, Member AIAA

[§] Research Scientist, Air Traffic Management Branch, Member AIAA

2 Nomenclature and Acronyms

A, B, C	Terminal sensitivity matrices
a	Speed of sound
C_L, C_D	Coefficients of lift and drag
D	Aerodynamic drag
$\vec{d}$	Disturbances vector
F	Equations of motion
G	Constraint equations (control equations)
h_i, h_p	Altitude (geometric, pressure)
i_e	Engine incidence angle
L	Aerodynamic lift
M	Mach number
m	Total aircraft mass
N	Output equations
p	Static air pressure
$\vec{p}$	Parametric error vector
S	Reference wing area
T	Engine thrust
t	Time
$\vec{u}$	Control vector
$\vec{V}_t$	True airspeed vector
$\vec{V}_i$	Inertial Velocity vector
V_{CAS}	Calibrated airspeed
V_g	Ground speed
W_x	Easterly component of wind
W_y	Northerly component of wind
W_h	Vertical component of wind
W_l	Horizontal component of wind
W_V	Wind component in velocity direction
W_Ψ	Wind component in lateral velocity direction
W_γ	Wind component in vertical velocity direction
$\vec{x}, \vec{y}$	State and output vectors
x_i, y_i	East and North positions

α	Angle of attack
α_t	Angle between thrust and relative wind
ε	Parametric variations in model
π	Engine control variable (E.G. EPR, PLA, N1)
γ_a	Flight path angle (relative to air mass)
γ_i	Flight path angle (relative to ground)
ψ	Segment termination condition
Θ, Φ	Segment transition matrices
Ψ_a	Velocity Heading (relative to air mass)
Ψ_i	Velocity Heading (relative to ground)
Ψ_w	Wind direction
ϕ	Bank Angle
CTAS	Center-TRACON Automation System
FMS	Flight Management System
TRACON	Terminal Radar Approach Control

3 Introduction

Increase in nation-wide air travel has put severe burdens on the current air traffic control system and controller's workload. It has become increasingly important to develop computerized automation to assist air traffic controllers.

Over the last decade, researchers at NASA Ames Research Center have designed and tested an air traffic control automation system, called Center-TRACON Automation System (CTAS). CTAS generates and displays descent advisories for air traffic controllers. Following these advisories, aircraft can descend efficiently, land in a scheduled order, and avoid potential conflict.

In essence, an air traffic control automation system, such as CTAS, consists of a scheduling tool and a trajectory synthesizing tool. Trajectory synthesis computes flight trajectories for many aircraft. These trajectories must be consistent with the air traffic control regulations and pilot procedures. They are efficient, conflict-free, and meet scheduled times of arrival. Based on these trajectories, the scheduler generates an efficient landing order and landing times. Finally, the ATC automation system extracts advisories from these trajectories for each aircraft in terms of heading, speed, and altitude. Therefore, trajectory synthesis is a core element to air traffic control automation.

Trajectory synthesis uses models of aircraft performance and weather conditions. These models necessarily contain errors from various sources. As a result, computed trajectories are different from aircraft trajectories flown in actual conditions. Because computed trajectories are used in conflict probing and scheduling, it is crucial to estimate the range of differences between computed trajectories and actual trajectories caused by modeling errors.

This paper presents an efficient approach for analyzing these differences. In this paper, pilot feedback controls are expressed as equality constraints that follow ATC and pilot procedures. Aircraft trajectories consist of a sequence of flight segments defined by changing control objectives and segment termination conditions. Various sources of errors are examined and described by either uncertain parameters or uncertain functions. A constrained linearization approach is developed for a complete descent profile similar to profiles used in the CTAS system. As a result, trajectory differences are governed by a set of linear, time-varying, ordinary differential equations with expressions that account for the change in segment transition times. The proposed method offers physical insight into the effects of various modeling errors and is computationally efficient.

In the rest of the paper, three-dimensional point-mass aircraft equations are first presented. Different components of the trajectory differences are analyzed, followed by discussions of mathematical representations by trajectory states, controls, and modeling errors. Then, theories of constrained linearization are developed. The use of constrained linearization is demonstrated with an example of a Boeing 757 descent. Time histories of trajectory error are demonstrated for a drag modeling error.

4 Equations of Motion

The point mass aircraft equations of motion with a dynamic wind environment are listed below. The equations of motion are written in the air-mass relative frame of reference, with the kinematic equations written in the inertial frame of reference.

$$\dot{V}_t = \frac{T\cos\alpha_t - D}{m} - g\sin\gamma_a - \dot{W}_V$$

$$\dot{\Psi}_a = \frac{(T\sin\alpha_t + L)\sin\phi}{mV_t\cos\gamma_a} + \frac{\dot{W}_\Psi}{V_t\cos\gamma_a}$$

$$\dot{\gamma}_a = \frac{(T\sin\alpha_t + L)\cos\phi}{mV_t}$$

$$
\begin{aligned}
& -\frac{g\cos\gamma_a}{V_t} + \frac{1}{V_t}\dot{W}_\gamma \\
\dot{x}_i &= V_t\cos\gamma_a\sin\Psi_a - W_l\sin\Psi_w \\
\dot{y}_i &= V_t\cos\gamma_a\cos\Psi_a - W_l\cos\Psi_w \\
\dot{h}_i &= V_t\sin\gamma_a + W_h \\
\dot{m} &= -\dot{m}_f
\end{aligned}
$$

where,

$$
\begin{aligned}
\alpha_t &= \alpha + i_e \\
W_l &= \sqrt{W_x^2 + W_y^2}
\end{aligned}
$$

Other quantities of interest can be represented as functions of the state variables.

$$
\begin{aligned}
M &= V_t/a(h_i) \\
\frac{V_{CAS}^2}{5a_{sl}^2} &= \left[\frac{p(h_i)}{p_{sl}}\left(\left[\frac{M^2}{5}+1\right]^{\frac{7}{2}}-1\right)+1\right]^{\frac{2}{7}}-1 \\
V_i &= \left(\dot{x}_i^2+\dot{y}_i^2+\dot{h}_i^2\right)^{\frac{1}{2}}
\end{aligned}
$$

The aerodynamic and propulsive forces are functions of the states and the control variables C_L, π.

$$
\begin{aligned}
L &= \frac{1}{2}\rho(h)V_t^2SC_L \\
D &= \frac{1}{2}\rho(h)V_t^2SC_D(C_L,M) \\
T &= T(\pi,h_p,M,\Delta ISA) \\
\dot{m}_f &= \dot{m}_f(\pi,h_p,M,\Delta ISA)
\end{aligned}
$$

The equations of motion form a 7 state system (V_t, Ψ_a, γ_a, x_i, y_i, h_i, m) with 3 control variables (C_L, π, ϕ). The other quantities of interest are represented as functions of the state variables and are considered to be outputs of the system of dynamic system.

5 Trajectory Deviations

All error sources that cause predicted aircraft trajectories to deviate from actual flown trajectories can be organized into the following six categories.

1. Theoretical approximations
2. Numerical approximations
3. Modeling errors
4. Measurement errors on the ground
5. Measurement errors on the airplane
6. Tracking properties of the pilot, autopilot, or Flight Management System.

Many of the error sources can be incorporated into the equations of motion as additional inputs to the system of equations. The inputs that represent these errors sources are categorized by whether the error is constant over the course of the flight, or varies. The constant error sources will be collected in a vector called $\vec{p}$, and the varying error sources in $\vec{d}(t)$.

Figure 1 illustrates the definition of four different trajectories. $\tilde{y}_{TS}$ represents a trajectory computed by numerical integration of the TS equations. y_{TS} represents the theoretical trajectory described by the TS equations of motion. y_o represents a reference aircraft trajectory found by integrating the point mass equations of motion with no other errors introduced. Finally, y represents the actual aircraft trajectory described by the point mass equations of motion with all error sources introduced.

The deviations between these 4 trajectories will be studied independently, with this paper focusing on the deviation caused by external error sources.

1. Errors due to external error sources
2. Errors due to different sets of equations
3. Numerical integration errors

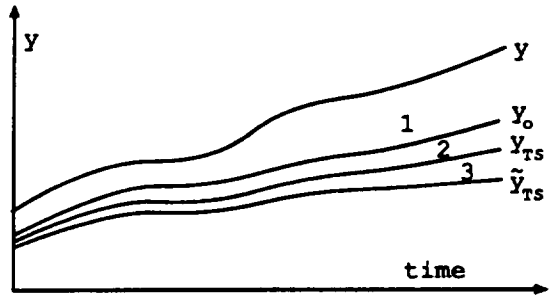

Figure 1: Components of Trajectory Deviations

For a more detailed description of error sources and components of trajectory deviations, see Reference [1].

6 Trajectory Representation

In both actual flight and in trajectory predictions using FMS and TS algorithms, a complete trajectory is divided into a series of segments. The segments are defined by 2 control objectives for the longitudinal motion, and 1 control objective for the lateral motion. The 2 longitudinal control objectives are chosen from 3 groups of objectives: speed (Mach number, CAS), vertical path (altitude, altitude rate, flight path angle), or throttle setting.

The flight segment transitions are determined by segment termination conditions, or "capture conditions". Typical capture conditions are altitude, CAS, Mach, and path distance.

The system of equations is represented symbolically by collecting the states, controls, inputs, outputs, and error sources into vectors.

$$\begin{aligned}
\vec{x} &= [V_t, \Psi_a, \gamma_a, x_i, y_i, h_i, m, t]' \\
\vec{u} &= [\pi, C_L, \phi]' \\
\vec{y} &= [V_{CAS}, \dot{V}_{CAS}, M, \dot{M}, \Psi_i, \dot{\Psi}_i, \gamma_i, \dot{\gamma}_i, V_g, V_i, \\
&\qquad h_p, \dot{h}_p, \ddot{h}_p, \ddot{h}_i, \dddot{V}_t, \dddot{V}_{CAS}, T]' \\
\vec{d} &= [\Delta W_x, \Delta W_y, \Delta W_h]' \\
\vec{p} &= [\Delta \vec{x}_{ic}, \varepsilon_{IT}, \varepsilon_{C_D}, \varepsilon_\tau, \varepsilon_{psl}, \varepsilon_{wind}, \\
&\qquad \Delta V_c, \Delta M_c, \Delta h_c, \Delta x_{TOD}]'
\end{aligned}$$

The perturbed equations of motion can be represented by the system of equations:

$$\begin{aligned}
\dot{\vec{x}} &= \vec{F}(\vec{x}, \vec{u}, \vec{d}, \vec{p}) && (1) \\
\vec{x}(t_{ic}) &= \vec{x}_{ic} + \Delta \vec{x}_{ic} && (2) \\
\vec{0} &= \vec{G}(\vec{x}, \vec{u}, \vec{d}, \vec{p}, t) && (3) \\
0 &= \psi(\vec{x}(t_i), \vec{p}, t_i) && (4) \\
\vec{y} &= \vec{N}(\vec{x}, \vec{u}, \vec{d}, \vec{p}) && (5)
\end{aligned}$$

7 Constrained Linearization

Define the reference trajectory, $x_o(t)$ by choosing: $\vec{d} = \vec{0}$, $\vec{p} = \vec{0}$, $\Delta \vec{x}_{ic} = \vec{0}$.

$$\begin{aligned}
\dot{\vec{x}}_o &= \vec{F}(\vec{x}_o, \vec{u}_o, \vec{0}, \vec{0}) && (6) \\
\vec{x}_o(t_{ic}) &= \vec{x}_{ic} && (7) \\
\vec{0} &= \vec{G}(\vec{x}_o, \vec{u}_o, \vec{0}, \vec{0}, t) && (8) \\
0 &= \psi(\vec{x}_o(t_f), \vec{0}, t_f) && (9) \\
\vec{y}_o &= \vec{H}(\vec{x}_o, \vec{u}_o, \vec{0}, \vec{0}) && (10)
\end{aligned}$$

These equations of motion are integrated segment by segment to obtain a reference trajectory. The segment transition times are denoted $t_1, t_2, \ldots,$ and the end of the trajectory by t_f.

The state variation is defined at a fixed point in time by the difference between the reference trajectory and the perturbed trajectory.

$$\delta \vec{x}(t) \equiv x(t) - x_o(t) \qquad (11)$$

The equations of motion are linearized by evaluating the first variation, in the sense of the calculus of variations.

$$\begin{aligned}
\delta \dot{\vec{x}} &= F_x \delta \vec{x} + F_u \delta \vec{u} + F_d \vec{d} + F_p \vec{p} && (12) \\
\vec{0} &= G_x \delta \vec{x} + G_u \delta \vec{u} + G_d \vec{d} + G_p \vec{p} && (13)
\end{aligned}$$

Since the constraint equations have been chosen to be well behaved, Equation (13) can be solved for the perturbed controls.

$$\delta \vec{u} = -G_u^{-1} \left(G_x \delta \vec{x} + G_d \vec{d} + G_p \vec{p} \right) \qquad (14)$$

Substituting (14) into (12) and collecting terms:

$$\begin{aligned}
\delta \dot{\vec{x}} &= (F_x - F_u G_u^{-1} G_x) \delta \vec{x} \\
&\quad + (F_d - F_u G_u^{-1} G_d) \vec{d} \\
&\quad + (F_p - F_u G_u^{-1} G_p) \vec{p} \\
\delta \dot{\vec{x}} &= \bar{F}_x \delta \vec{x} + \bar{F}_d \vec{d} + \bar{F}_p \vec{p} && (15) \\
\text{where :} \quad & \bar{F}_x \equiv F_x - F_u G_u^{-1} G_x \ , \text{ etc.}
\end{aligned}$$

The output variation is found in a similar fashion.

$$\delta \vec{y} = \bar{N}_x \delta \vec{x} + \bar{N}_d \vec{d} + \bar{N}_p \vec{p} \qquad (16)$$

The above linearized system is defined at each point in time along the reference trajectory, with the equations changing discontinuously at the segment transitions. Additionally, the segment transition times will vary as the trajectory is perturbed.

Define the state differential $dx(t_i)$ as the difference between $x_o(t_i)$ and $x(t_i + dt_i)$, the state at the i'th reference transition at time t_i and the state at the perturbed transition at time $t_i + dt_i$. Since the equations change at time t_i, the distinction will be

made below whether the values are before (t_i^-) or after (t_i^+) the transition.

$$\begin{aligned} dx(t_i) &\equiv x(t_i + dt_i) - x_o(t_i) \\ &= x(t_i^-) + \dot{x}(t_i^-)dt_i - x_o(t_i) \\ &= \delta\vec{x}(t_i^-) + \bar{F}(t_i^-)dt_i \quad (17) \\ &= \delta\vec{x}(t_i^+) + \bar{F}(t_i^+)dt_i \quad (18) \end{aligned}$$

where, $\bar{F}(t) \equiv \bar{F}(x, p, d, t) \equiv \frac{dx}{dt}\big|_{G=0}$. See Figure 2.

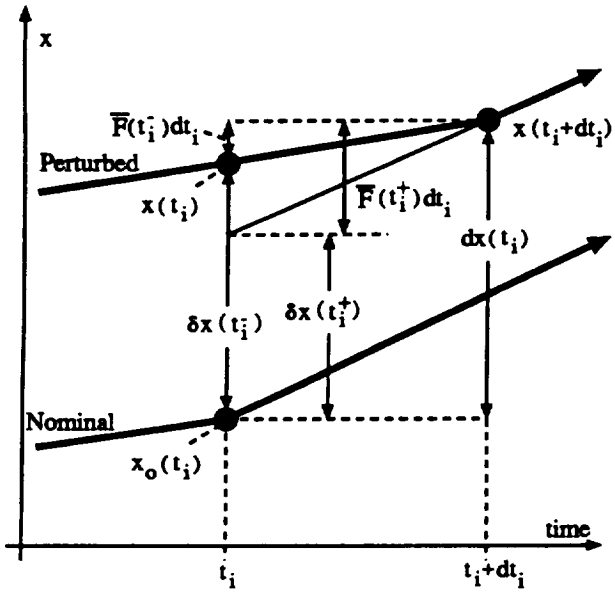

Figure 2: Errors During Segment Transition

The differential of the capture condition must be zero to ensure that it is satisfied at the perturbed transition time. This will require a differential in the segment transition time to satisfy the capture condition.

$$\begin{aligned} d\psi_i &= \frac{\partial\psi_i}{\partial x}d\vec{x}(t_{i+1}) + \frac{\partial\psi_i}{\partial p}\vec{p} + \frac{\partial\psi_i}{\partial t}dt_{i+1} \\ &= \frac{\partial\psi_i}{\partial x}\delta\vec{x}(t_{i+1}^-) + \frac{\partial\psi_i}{\partial p}\vec{p} \\ &\quad + \left(\frac{\partial\psi_i}{\partial x}\bar{F}(t_{i+1}^-) + \frac{\partial\psi_i}{\partial t}\right)dt_{i+1} \\ &= \frac{\partial\psi_i}{\partial x}\delta\vec{x}(t_{i+1}^-) + \frac{\partial\psi_i}{\partial p}\vec{p} + \dot{\psi}_i dt_{i+1} = 0 \\ &\quad \text{where, } \dot{\psi}_i = \frac{\partial\psi_i}{\partial x}\bar{F}(t_{i+1}^-) + \frac{\partial\psi_i}{\partial t} \end{aligned}$$

Solving for the differential in segment transition time:

$$dt_{i+1} = -\dot{\psi}_i^{-1}\left[\frac{\partial\psi_i}{\partial x}\delta\vec{x}(t_{i+1}^-) + \frac{\partial\psi_i}{\partial p}\vec{p}\right] \quad (19)$$

The portion of the perturbed trajectory with a light line in Figure 2, between the reference transition time (t_i) and the actual transition time ($t_i + dt_i$), is fictitious but is required later for the expressions for terminal error. This segment is required since the time differential is allowed to be arbitrary. This fictitious trajectory segment could be removed for the time histories of trajectory error, but since this is not the main purpose of the method, that is not described.

Equations (15) and (16) represent a linear dynamic system with time varying coefficients that describe the response of the trajectory errors to the disturbances, with transitions between segments described by equations (17), (18) and (19). The following section will discuss various uses of this system to analyze the trajectory sensitivities.

The method of Constrained Linearization can be formulated with any appropriate independent variable instead of time, such as path distance.

8 Uses of the Linearized System

8.1 Trajectory Error History

The linear time varying system that describes the trajectory errors can be integrated across each segment from the initial conditions at time t_o to time t_f.

$$\begin{aligned} \delta\vec{x}(t) &= \delta\vec{x}(t_o) + \sum_{i=1}^{n(t)}[\delta\vec{x}(t_i^+) - \delta\vec{x}(t_i^-)] \\ &\quad + \int_{t_o}^{t}\left(\bar{F}_x\delta\vec{x} + \bar{F}_d\vec{d} + \bar{F}_p\vec{p}\right)dt \quad (20) \end{aligned}$$

This can be integrated to determine the variation in the state history. The summation terms account for the change in the closed loop state equations across the segment transitions combined with the differential in the transition time. $n(t)$ represents the number of transitions that have been encountered through time t. Substituting the definition of $\delta\vec{x}$ from Equations (17) and (18):

$$\begin{aligned} \delta\vec{x}(t) &= dx(t_o) - \bar{F}(t_o)dt_o \\ &\quad + \sum_{i=1}^{n(t)}[\bar{F}(t_i^+) - \bar{F}(t_i^-)]dt_i \end{aligned}$$

$$+ \int_{t_i}^{t} \left(\bar{F}_x \delta\vec{x} + \bar{F}_d \vec{d} + \bar{F}_p \vec{p} \right) dt \quad (21)$$

Note that the integration occurs from the reference initial time t_o to the reference final time t_f, with each segment being integrated from t_i to t_{i+1}, since the state variations across the segment transitions due to the transition time differences are accounted for by the $\bar{F} dt_i$ terms. (See Figure 2.)

The differential in the final state can be found from Equation (17).

$$dx(t_f) = \delta\vec{x}(t_f^-) + \bar{F}(t_f^-) dt_f \quad (22)$$

8.2 Expressions for Terminal Error

It is valuable to have expressions for the terminal error that do not require integrating the full linear time varying system for each set of disturbances and parameters chosen. This section describes an expression for the error at the end of a single segment based on the conditions at the beginning of the segment and the errors introduced during the segment. This method is then extended for multi-segment trajectories by accounting for the change in errors across the segment transitions.

Evaluating Equation (20) from an initial time t_i to a final time t_{i+1}:

$$\begin{aligned} \delta\vec{x}(t_{i+1}^-) &= \delta\vec{x}(t_i^+) \\ &+ \int_{t_i}^{t_{i+1}} \left(\bar{F}_x \delta\vec{x} + \bar{F}_d \vec{d} + \bar{F}_p \vec{p} \right) dt \end{aligned}$$

To obtain an expression for the final state variation in terms of only the disturbances and parameters, the state variation in the integrand of the above equation must be eliminated. This will be accomplished by adjoining the integrand with a Lagrange multiplier matrix Λ times the state error evolution equation. This does not change the integral, since the state equation is always zero, but is a trick that can be used to simplify the problem. The Lagrange multiplier will be chosen to eliminate $\delta\vec{x}$ in the integrand.

$$\begin{aligned} \delta\vec{x}(t_{i+1}^-) &= \delta\vec{x}(t_i^+) \\ &+ \int_{t_i}^{t_{i+1}} \left[\bar{F}_x \delta\vec{x} + \bar{F}_d \vec{d} + \bar{F}_p \vec{p} \right. \\ &+ \left. \Lambda(\bar{F}_x \delta\vec{x} + \bar{F}_d \vec{d} + \bar{F}_p \vec{p} - \delta\dot{\vec{x}}) \right] dt \end{aligned}$$

Integrating by parts and collecting terms.

$$\begin{aligned} \delta\vec{x}(t_{i+1}^-) &= \delta\vec{x}(t_i^+) \quad (23) \\ &- \Lambda(t_{i+1}^-)\delta\vec{x}(t_{i+1}^-) + \Lambda(t_i^+)\delta\vec{x}(t_i^+) \\ &+ \int_{t_i}^{t_{i+1}} \left[\left((I+\Lambda)\bar{F}_x + \dot{\Lambda} \right) \delta\vec{x} \right. \\ &+ \left. (I+\Lambda)\bar{F}_d \vec{d} + (I+\Lambda)\bar{F}_p \vec{p} \right] dt \end{aligned}$$

Choose : $\Lambda(t_{i+1}^-) = 0 \quad (24)$

$$\dot{\Lambda} = -(I+\Lambda)\bar{F}_x \quad (25)$$

Λ can be integrated backwards in time as a function of the reference trajectory alone – independent of the variations in the initial and final conditions, and the disturbances and parameters. A physical interpretation of Λ is the sensitivity of the final state to a variation in the current state derivative. $\Lambda(t) = \frac{\partial x(t_{i+1})}{\partial \dot{x}(t)}$

Substituting Equations (24) and (25) into (23), and gathering terms, the state variation at time t_{i+1}^- is:

$$\begin{aligned} \delta\vec{x}(t_{i+1}^-) &= a_i \, \delta\vec{x}(t_i^+) + c_i \, \vec{p} \\ &+ \int_{t_i}^{t_{i+1}} b_i(t)\vec{d}(t) \, dt \quad (26) \end{aligned}$$

where:

$$a_i = (I + \Lambda(t_i^+)) \quad (27)$$

$$b_i(t) = (I+\Lambda)\bar{F}_d \quad (28)$$

$$c_i = \int_{t_i}^{t_{i+1}} (I+\Lambda)\bar{F}_p dt \quad (29)$$

The variation in the final state at the final time is not the desired answer, since a differential in final state is required to satisfy the terminal condition. For a single segment trajectory, or the final segment of a multi-segment trajectory, the final state differential is found by extrapolating along the trajectory for the time differential dt_{i+1} (19).

$$dx(t_{i+1}) = \delta\vec{x}(t_{i+1}^-) + \bar{F}(t_{i+1}^-) dt_{i+1}$$

$$\begin{aligned} dx(t_{i+1}) &= \left(I - \bar{F}(t_{i+1}^-)\dot{\psi}_i^{-1} \frac{\partial \psi_i}{\partial x} \right) \delta\vec{x}(t_{i+1}^-) \\ &\quad - \bar{F}(t_{i+1}^-)\dot{\psi}_i^{-1} \frac{\partial \psi_i}{\partial p} \vec{p} \end{aligned}$$

$$\Phi_i = I - \bar{F}(t_{i+1}^-)\dot{\psi}_i^{-1} \frac{\partial \psi_i}{\partial x} \quad (30)$$

$$\Theta_i = -\bar{F}(t_{i+1}^-)\dot{\psi}_i^{-1} \frac{\partial \psi_i}{\partial p} \quad (31)$$

$$dx(t_{i+1}) = \Phi_i \, \delta\vec{x}(t_{i+1}^-) + \Theta_i \, \vec{p} \quad (32)$$

The matrix Φ_i can be interpreted as taking the variation in state at the final time along the constrained equations of motion until the terminal condition is met. The matrix Θ_i can be interpreted as the change in final state due to a perturbation of the termination condition ψ.

Substituting Equation (26) into (32), and simplifying the result.

$$d\boldsymbol{x}(t_{i+1}) = A_i\, \delta\vec{x}(t_i^+) + C_i\vec{p} + \int_{t_i}^{t_{i+1}} B_i(t)\vec{d}(t)\, dt \qquad (33)$$

where:

$$A_i = \Phi_i\, a_i \qquad (34)$$

$$B_i(t) = \Phi_i\, b_i(t) \qquad (35)$$

$$C_i = \Phi_i\, c_i + \Theta_i \qquad (36)$$

For a segment transition, the errors are extrapolated from the end of the first segment to the perturbed transition time, then back to the reference transition time. Equating Expressions (17), (18) at time t_{i+1}, substituting Equation (19), and solving for $\delta\vec{x}(t_{i+1}^+)$ yields:

$$\delta\vec{x}(t_{i+1}^+) = \Phi_i\, \delta\vec{x}(t_{i+1}^-) + \Theta_i\, \vec{p}$$

$$\Phi_i = I + \left(\bar{F}(t_{i+1}^+) - \bar{F}(t_{i+1}^-)\right) \dot{\psi}_i^{-1} \frac{\partial \psi_i}{\partial x}$$

$$\Theta_i = \left(\bar{F}(t_{i+1}^+) - \bar{F}(t_{i+1}^-)\right) \dot{\psi}_i^{-1} \frac{\partial \psi_i}{\partial p}$$

$$\delta\vec{x}(t_{i+1}^+) = A_i\, \delta\vec{x}(t_i^+) + C_i\vec{p} + \int_{t_i}^{t_{i+1}} B_i(t)\vec{d}(t)\, dt$$

where, A_i, B_i, C_i are found from Equations (34) - (36).

Extending the result to multiple segments:

$$A_i = \Phi_i\, a_i\, A_{i-1}$$

$$B_i(t) = \Phi_i\, (b_i(t) + a_i B_{i-1})$$

$$C_i = \Phi_i\, (c_i + a_i C_{i-1}) + \Theta_i$$

The expressions A, $B(t)$, and C can be interpreted as the influence functions of the initial conditions, disturbances, and parameters on the final state differential. The influence functions provide a quantification of the effects of the error sources on the final state differential. The influence functions A and C can be interpreted directly as the sensitivity of the final states to the initial conditions and parameters. $B(t)$ can be examined as a function of time to observe when the trajectory is most sensitive to the disturbances, or integrated with a given disturbance history $\vec{d}(t)$ to obtain the total error due to a particular disturbance.

8.3 Worst Case Disturbances

The influence function $B(t)$ indicates the influence of the disturbances at a point in time on the final states. This influence function can be used at each point in time to select a worst case disturbance to drive the final state error in a particular direction. For example, the disturbance vector may be magnitude limited and we are interested in what is the worst case error for any disturbance that meets this condition. The product of $B(t)$ and the so chosen worst case disturbance $\vec{d}(t)$ can be integrated to obtain an estimate of the worst case errors for a given class of disturbances.

8.4 Covariance Analysis

The linear time varying system lends itself well to the analysis of random disturbances using covariance analysis. This analysis provides the standard deviation of the state error as a function of time given statistical properties of the disturbances.

Bryson and Ho, [13] pages 342-345, describe a method of covariance analysis for a linear time varying system with random noise inputs.

A method to account for the covariance propagation across segment transitions is under development.

9 Example Application

An example is presented for a descent trajectory with a flight profile similar to a CTAS descent through an Approach Control Center airspace. The aircraft model used is the CTAS Boeing 757 model. The reference trajectory is define by the sequence of flight segments described in Table 1 below. Also shown in Table 1 are the segment transition conditions, the times the transitions occur, and the

changes to the transition times due to a drag perturbation. The reference trajectory is shown in Figure 3.

The trajectory deviation due to a modeling error in drag of 5% is shown in Figure 4, as computed by the method described in Section 8.1.

The sensitivity of the final states of the reference trajectory to the initial conditions and parametric error sources can be computed directly from the trajectory as described in Section 8.2. Table 2 shows selected columns from the matrix A and Table 3 shows the matrix C. The columns of both tables have been scaled by reasonable magnitudes of the error sources for a better comparison of relative importance of trajectory error due to the error sources. Note that the reference trajectory ends in a level flight segment at specified airspeed and inertial position, so the final state errors are absorbed primarily in the final time. The idle thrust perturbation is between the nominal model of idle thrust and zero idle thrust at all flight conditions.

10 Conclusions

This paper develops a constrained linearization approach for the analysis of differences between computed and actual aircraft trajectories in air traffic control automation. Synthesized trajectories are needed in ATC automation to predict aircraft flight paths. Due to the modeling errors in trajectory computations, synthetic trajectories are different from actual trajectories. In this paper, modeling errors are described with uncertain parameters and uncertain functions. Pilot feedback control actions are expressed as equality constraints along a flight path. A constrained linearization approach is developed to analyze trajectory perturbations along a reference path caused by modeling errors. A numerical example is presented to illustrate the applications of the proposed techniques. The example demonstrates the efficiency and physical insight offered by the proposed approach.

11 Acknowledgments

This work is supported by NASA Ames Research Center under NCC2-868, and also by Honeywell Internal Research and Development.

References

[1] Yiyuan Zhao, Michael R. C. Jackson, Rhonda A. Slattery, "Aircraft Trajectory Sensitivities in Air Traffic Control Automation and Flight Management", AIAA Guidance, Navigation and Control Conference, pp 1467-1473, 1995.

[2] Michael R. C. Jackson, "Sensitivities of Aircraft Trajectories for Air Traffic Control Automation and Flight Management Systems", PhD Thesis in progress, University of Minnesota, to be completed in the Fall of 1996.

[3] Heinz Erzberger, Thomas J. Davis, and Steve Green, "Design of Center-TRACON Automation System," presented at the AGARD Guidance and Control Symposium on *Machine Intelligence in Air Traffic Management*, 11-14 May 1993, Berlin, Germany.

[4] Heinz Erzberger and L. Tobias, "A Time-Based Concept for Terminal-Area Traffic Management," NASA TM 88243, April 1986.

[5] Heinz Erzberger, "Automation of On-Board Flightpath Management," NASA TM 84212, December 1981.

[6] Rhonda Slattery, Yiyuan Zhao, "En-Route Descent Trajectory Synthesis for Air Traffic Control Automation", American Control Conference, 1995.

[7] Robert L. Schultz, "Three-Dimensional Trajectory Optimization for Aircraft", *Journal of Guidance, Control, and Dynamics*, Nov-Dec 1990, pp 936-943.

[8] Robert L. Schultz, "Advanced Air Traffic Control and Flight Management System Concepts," AGARD-CP-538, 14 May 1993.

[9] David Williams, "Fuel Penalties and Time Flexibility of 4D Flight Profiles Under Mismodeled Wind Conditions," NASA TM-89128, March 1987.

[10] David Williams , "Impact of Mismodeled Idle Engine Performance on Calculation and Tracking of Optimal 4D Descent Trajectories", American Control Conference, 1986, pp 681-686.

[11] J.A. Sorenson, M.H. Waters, "Generation of optimum vertical profiles for an advanced flight management system," NASA CR-165674, March 1981

[12] George Hunter, Richard Bortins, "CTAS Error Sensitivity Study: Analysis Plan", Seagull TM 95133-02, June 1995.

[13] Arthur E. Bryson, Yu-Chi Ho, "Applied Optimal Control", Hemisphere Publishing, 1975.

[14] John D. Anderson, *Introduction to Flight*, third edition, McGraw-Hill, 1978, p. 121.

[15] Yiyuan Zhao, and Rhonda Slattery, "Capture Conditions in Center Trajectory Synthesizer for Center-TRACON Automation System," AIAA Guidance and Control Conference, August 7-9, 1995.

Seg #	Control Obj. 1	Control Obj. 2	Capture Cond.	End Time	Time Diff
1	$h_p = 35000$ ft	$M = 0.78$	$x_i = 70$ nm	560.8 sec	0 sec
2	$M = 0.78$	$\pi = idle$	$V_{CAS} = 307$ knt	678.4 sec	-5.6 sec
3	$V_{CAS} = 310$ knt	$\pi = idle$	$h_p = 10400$ ft	1094.0 sec	-26.9 sec
4	$h_p = 10000$ ft	$\pi = idle$	$V_{CAS} = 250$ knt	1164.2 sec	-30.8 sec
5	$h_p = 10000$ ft	$V_{CAS} = 250$ knt	$x_i = 150$ nm	1312.3 sec	+12.5 sec

Table 1: Example Trajectory Description (A 757 Descent)

Final State Error		Initial State Error			
		V_t	x_i	h_i	mg
		1 knot	0.2 nmile	200 ft	7000 lbs
V_t	knots	0	0	0	0
γ_a	deg	0	0	0	0
x_i	nmile	0	0	0	0
h_i	feet	0	0	0	0
mg	lbs	1.08	2.80	5.72	7011.4
t_f	sec	-0.023	-1.60	0	-7.94

Table 2: Terminal Sensitivity to Initial Conditions

Final State Error		Parametric Error Source						
		Idle Thrust	Drag	Wind	V_{CAS_c}	M_c	h_{p_c}	x_{TOD}
		see text	+ 5 %	5 knots	2 knots	0.005	200 ft	2 nmiles
V_t	knot	0	0	0	2.27	0	0.854	0
γ_a	deg	0	0	0	0	0	0	0
x_i	nmile	0	0	0	0	0	0	0
h_i	feet	0	0	0	0	0	200	0
mg	lbs	-27.6	-101	-33.8	-10.3	-7.41	3.61	15.9
t_f	sec	2.0	12.5	19.3	-1.3	-4.51	-1.04	-8.9

Table 3: Terminal Sensitivity to Parametric Errors

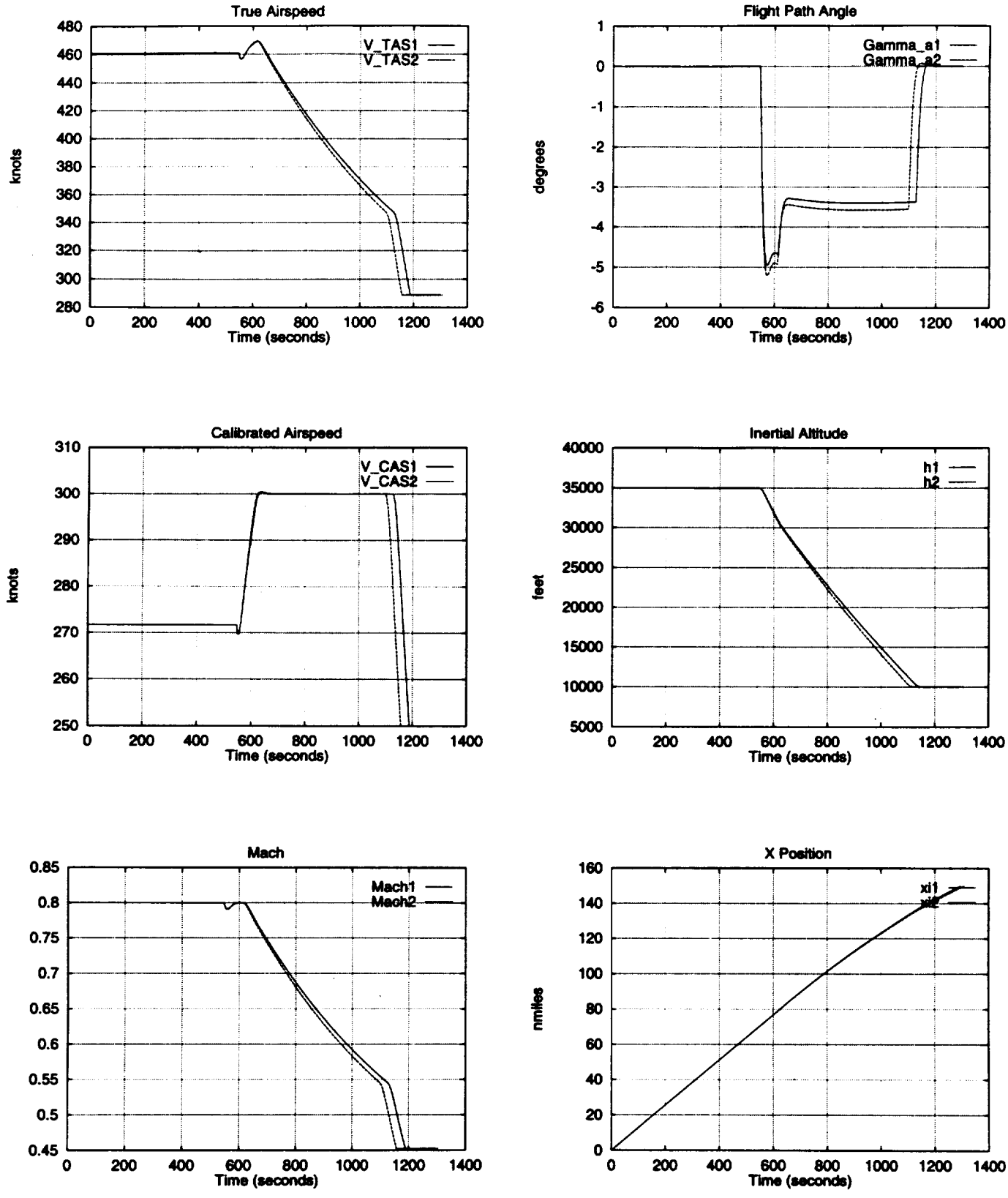

Figure 3: Boeing 757 Descent Reference Trajectory and Perturbed Trajectory

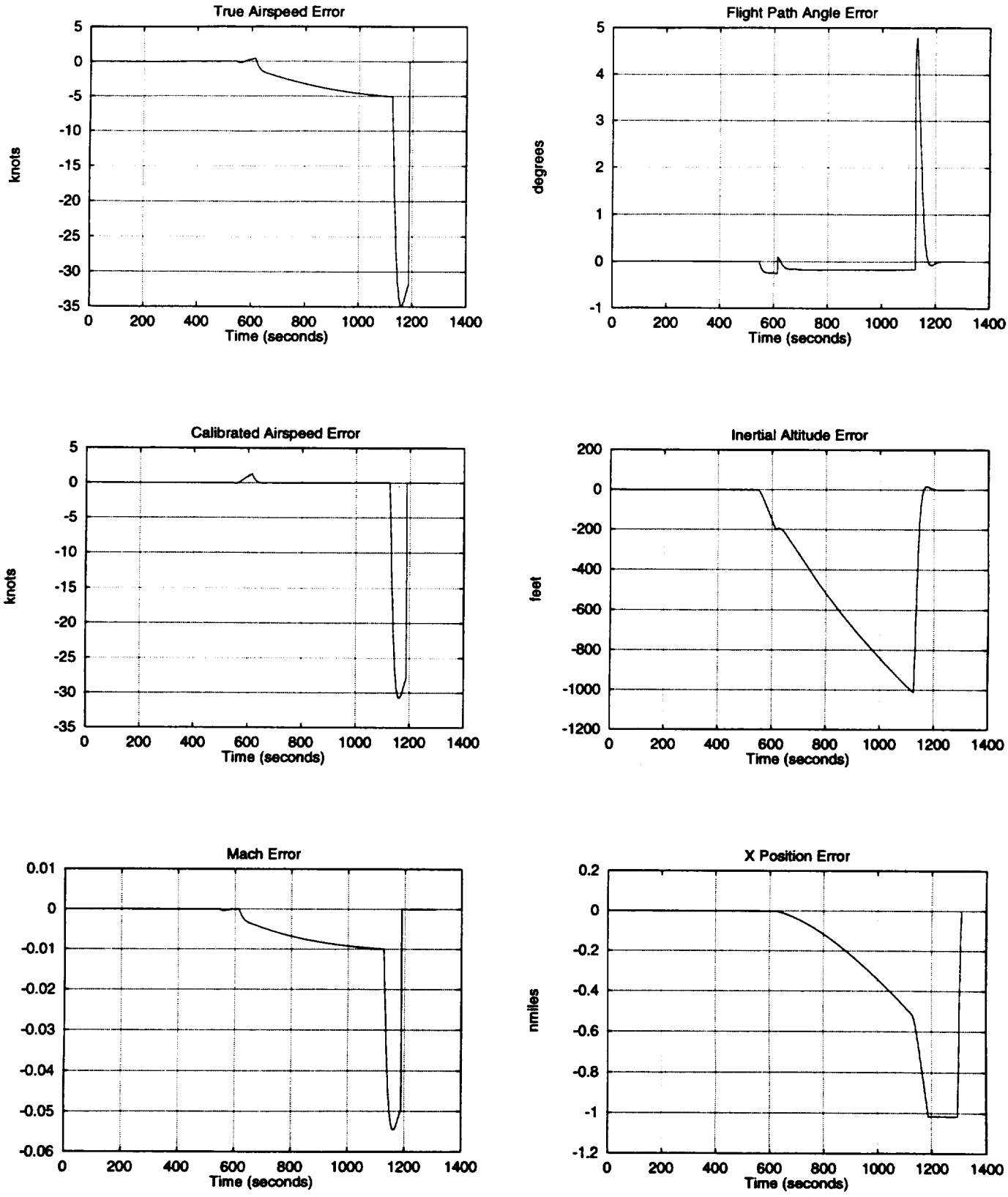

Figure 4: Trajectory Deviation Due to 5 % Drag Error